MIXED FILM COATINGS ANALYZED BY MICRO X-RAY FLUORESCENCE METHOD

M. LUNGU, C. DOBREA, T.CRACIUNESCU, I. TISEANU, C. POROSNICU[*],
I. JEPU, I. MUSTATA
National Institute for Laser, Plasma and Radiation Physics, Bucharest, Romania;

The purpose of this reported work is the analysis of nickel-based thermal barrier coatings prepared by thermionic vacuum arc method using the micro X-ray fluorescence (micro-XRF) technique. Atomic concentration calibration and comparison between theoretical and real distribution of the alloys composition in the obtained layers with thermal barrier properties are presented. 3D mapping of nickel, rhenium, and chromium surface relative concentrations was performed on a 240 mm x 90 mm substrate plate.

1. Introduction

Nickel based alloys, also called thermal barrier coatings (TBC) [1-2], are known to be highly efficient at elevated temperatures, having surface stability, corrosion and oxidation resistance. This fact makes them key elements in a wide range of applications like heat exchanger tubing, chemical processing vessels, military electric motors, nuclear reactors, space vehicles oil and gas industry applications [3].

Nickel-based alloys may contain materials such as ruthenium (Ru), rhenium (Re), titanium (Ti), cobalt (Co), chromium (Cr) and other elements. Alloys based on the mentioned materials are capable to exceed 1000 ^{o}C, the temperature barrier of ordinary steel [4].

The latest tendency in the development of TBC is to use expensive metals such as rhenium and ruthenium to achieve a new generation of progressive temperature resistance alloys.

The high operating temperature of the turbine system has a direct impact on its efficiency, output power and reduced emissions due to the completion of combustion cycle [5]. Nano-crystalline electro-deposited nickel-based TBC revealed an exothermic peak around 600 ^{o}C but not below this point [6]. This is determined by the heat-resistant property of the Re with its melting point around 3180 ^{o}C resulting a thermal stable improved Ni-Re alloy. For example, rhenium addition decreases the oxidation rate of the super-alloy coating and improves its mechanical properties [7]. An important aspect was to determine the accurate relative concentrations of Re and Ni in a certain coating order to improve the thermal barrier property of the alloys [8].

2. Sample preparation

The proposed method for obtaining TBC is thermionic vacuum arc (TVA)which is characterized by a high voltage (0.3-4 kV) low current (0.1- 4A) discharge ignited in the pure vapors of the metallic materials to be deposited. One significant advantage is the lack of any buffer gas inside the coating chamber [9-12].

---

* Corresponding author: corneliu.porosnicu@inflpr.ro

The evaporation of the desired metals (in our case Re, Ni, Cr) takes place in high vacuum conditions (about 10^{-4} Pa). An external heated tungsten (W) grounded cathode having 0.8-1.2 mm in diameter produces thermal electrons by a 20-60A current passing through it. These electrons are accelerated and focused through a Wehnelt cylinder towards the anode by the applied high voltage (0.3 – 4 kV). The electron beam focus is necessary to ensure melting and evaporation of the material's atoms. The high voltage also ensures the ionization of the evaporating atoms and the ignition of the electrical discharge. The ions are directed with high energies (200-1000 eV) towards the substrates, usually heated at 400°C. TVA plasma is localized within 5-10 cm from the anode-cathode system. This makes possible the ignition of multiple TVA sources simultaneously [13].

For this study, the specific deposition conditions of the preparation of TBC on a 240 mm x 90 mm glass substrate with Ni, Re and Cr mixed alloy are presented below:

The specific conditions of TVA method, for the preparation of thermal barrier coatings,

- Three anodes of Ni, Re and Cr were used to obtain the thermal barrier mixed alloy schematically shown in Fig. 1;

- The thicknesses of each material (Ni, Re, Cr) were individually monitored using three different quartz balances;

- The variation of the relative elemental relative concentrations at a certain coordinate on the glass substrate was controlled by the position of the substrate in respect with the anode-cathode system;

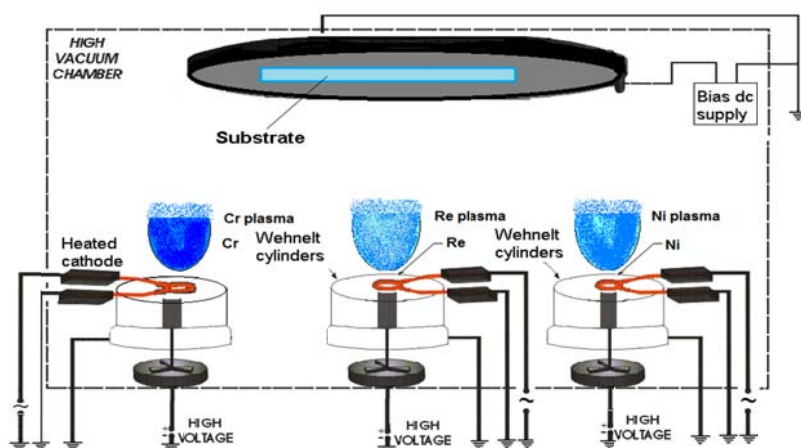- The discharge voltages and currents for every TVA sources were kept constant during depositions;

-

Fig. 1 The experimental setup of TVA method

The analysis for TBC layers obtained by TVA was performed using the Tomo-Analytic system, which was mainly developed in our laboratory for the fusion materials analysis [14-15]. The Tomo-Analytic system (http://tomography.inflpr.ro/) is a configurable and versatile tool in which different measuring techniques can be adapted in the characterization of the metallic coatings thickness uniformity.

Micro X-ray fluorescence (micro XRF) method used for film characterization has the following characteristics, special design and technical issues:

- The use of a policapillary lens with a focal spot in the range of few nanometers to hundreds of nanometers which improved the detection sensitivity [16] ;

- The locally measured peak intensities were converted to elemental atomic concentrations locally measured surface.
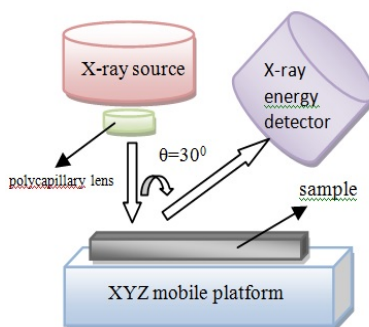
Fig. 2 Micro X-ray fluorescence principle

3. Theoretical and experimental distribution of the elemental concentrations using deposition by TVA and micro-XRF methods

In order to determine de deposition rate on the sample it is critical to take into account the fact that the deposition rate decreases with the square of the distance from the anode to the sample and depends on the incident angle of the atoms towards the substrate reported to the vertical point of evaporation [17].
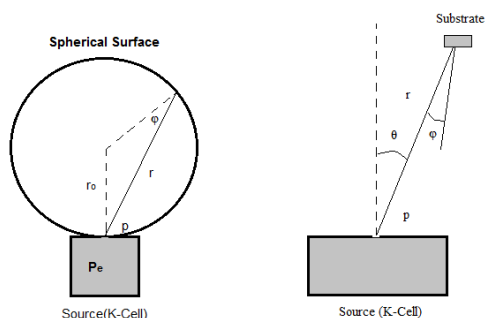

Fig. 3 Deposition geometry

The theoretical distribution can be calculated using the Langmuir-Knudsen formula [18]:

$$R_m = C_m \left(\frac{M}{T}\right)^{1/2} cos\theta cos\Phi \frac{1}{r^2}[P_e(T) - P] \tag{1}$$

where

$$P_e = C \cdot \exp\left(-\frac{w}{kT}\right) \tag{2}$$

and C_m is 0.0185 , r represents the source-sample distance (cm) , T is the anode temperature, P_e is the vapor pressure (Torr), P is the residual pressure in deposition chamber, M is the molar mass of the evaporator (g).

This relationship can be derived easily from the expression of the evaporation rate formula [18-19]:

$$\log \varphi = \log p + 22.546 – 0.5\log(MT) \tag{3}$$

with ϕ as evaporated flux given in mol/(cm^{2}sec), p pressure in Torr, T - temperature in Kelvin, M-molar mass, by adding the influence of inclination angle, θ and φ.

In practice, the deposition rates are estimated by this formula and the deposited layer's thicknesses are evaluated by the deposition time multiplied by the deposition rate and both are displayed on the measuring gauge screen.

Based on these calculations, a test sample was produced using simultaneously TVA discharges. The concentrations in a predefined position using calibration curves correlating thin film thickness with at/cm^2 concentration were measured. Using these comparisons the geometric correction factor for the real Re-Ni-Cr depositions was deducted.

For a simultaneous two components coating, in order to obtain depositions with equal particle number, we used the measurement gauge located next to deposition sample [17].

In the case of a binary co-deposition, composed of elements "1" and "2", the ratio of the "1" number of atoms to the total number of atoms is $\alpha. = v_1 / (v_2 + v_1) = v_1 / v$, where v_2 is the number of particles "2".

If ρ_1 and ρ_2 are the corresponding densities of the two materials, then the volumes occupied by an atom (molecule) of the two substances will be :

$$v_1 = 1/n_1 = m_1 / \rho_1 \text{ and } v_2 = 1/n_2 = m_2 / \rho_2 \qquad (4)$$

where $n_1 = \rho_1/m_1$ is the pure number of particles "1" per volume unit and normally it is not mixed and $n_2 = \rho_2/m_2$ particle number "2" on unit volume when not mixed.

A partial volume in cm^3 occupied by the element "1" and the element "2" within the desired mixture will be respectively:

$$\alpha v m_1 / \rho_1 \text{ and } (1 - \alpha) v m_2 / \rho_2 \qquad (5)$$

The sum of these volumes must be equal to unit volume:

$$\alpha v m_1 / \rho_1 + (1 - \alpha) v m_2 / \rho_2 = 1 \qquad (6)$$

From this relation, the total number of particles, υ present per unit volume is:

$$v = \frac{1}{\alpha \dfrac{m_1}{\rho_1} + (1-\alpha)\dfrac{m_2}{\rho_2}} \qquad (7)$$

Total weight of mixture per unit volume is:

$$\rho_{am} = [\alpha m_1 + (1-\alpha)m_2]v = \frac{\alpha m_1 + (1-\alpha)m_2}{\alpha \frac{m_1}{\rho_1} + (1-\alpha)\frac{m_2}{\rho_2}} = \frac{\rho_1\rho_2[\alpha m_1 + (1-\alpha)m_2]}{\alpha m_1\rho_2 + (1-\alpha)m_2\rho_1} \qquad (8)$$

If $\alpha = 1$ (present only the item "1"), it is observed that $\rho_{am} = \rho_1$ and if $\alpha = 0$ (present only the item "2"), then $\rho_{am} = \rho_2$.

The calculated average density (8) is introduced as software parameter when is performed the "in situ" measurement of thickness of the deposited layers.

Furthermore, a dependency between particles flow that arrive at the substrate creating the coating and the growth rates (given in thickness of layer mixture material deposited per unit time was obtained).

In this sense, the mass of substance "1" is $(v_1 / \tau) m_1 = S\rho_1 w_1$, where τ is the time of deposition, v_1 is the number of particle "1" arrived in time τ to the surface S of the deposition rates monitor and w_1 the deposition rate for substance "1". Same reasoning was made for substance "2". The number of particles "1" over the number of particle "2" arriving at the monitor in the time unit must be equal to $(v_1 / \tau) / (v_2 / \tau) = v_1/v_2 = \alpha / (1-\alpha)$ in order to have the desired mixture. Using the relations $(v_1 / \tau) m_1 = S\rho_1 w_1$ and $(v_2 / \tau) m_2 = w_2 S\rho_2$ it results $v_1 m_1 / (v_2 m_2) = \rho_1 w_1 / (\rho_2 w_2)$ and therefore $v_1/v_2 = [\rho_1 w_1 / (\rho_2 w_2)] (M_2/M_1) = \alpha / (1-\alpha)$.

Then, if the measured deposition rate for the item "1" is chosen to be w_1, then in order to obtain the desired mixture, the deposition rate for the item "2", must be:

$$w_2 = \frac{\rho_1 w_1 (1-\alpha) m_2}{\rho_2 \alpha m_1} \tag{9}$$

Total deposition speed must be:

$$w_1 + w_2 = w_1 \left[1 + \frac{\rho_1 (1-\alpha) m_2}{\rho_2 \alpha m_1} \right] \tag{10}$$

This two system deduction of density and deposition rates can be easily extended to ternary or higher systems [17].

Using the above considerations, the theoretical (at/cm^2) elemental (Ni, Re, Cr) distribution was calculated and plotted on a rectangular area of 240 mm x 90 mm.
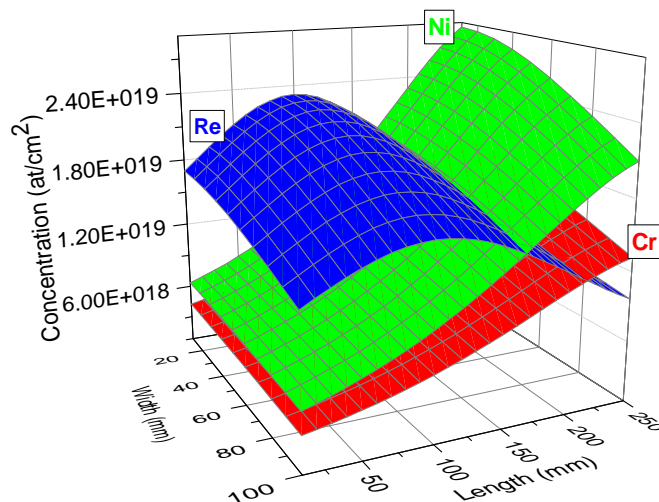

Fig. 4 Theoretical at/cm2 elemental (Ni, Re, Cr) distribution calculated and plotted on an area of 240 mm x 90 mm

In order to calibrate the micro-XRF measurements with the atomic concentration of the thin films, a set of Ni, Re and Cr samples with well known thicknesses were prepared. Silicon, graphite, glass and stainless steel were used as substrates. The film thickness was monitored "in situ" using micro quartz balances devices. After the deposition process, a stylus profilometer was used to confirm the films thickness. The matching calibration curves of Ni, Re and Cr bond the relations between the photon counts of the detector and the atomic concentration of the pure thin films, as shown in Figs. 5-7.
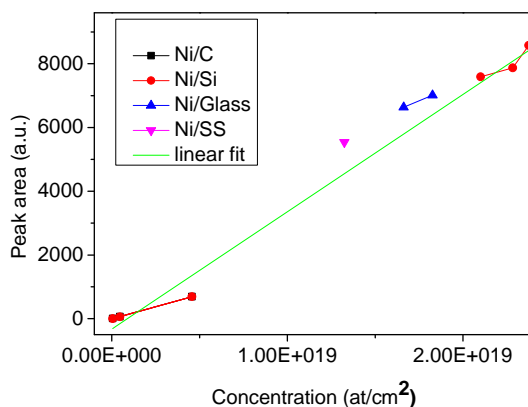

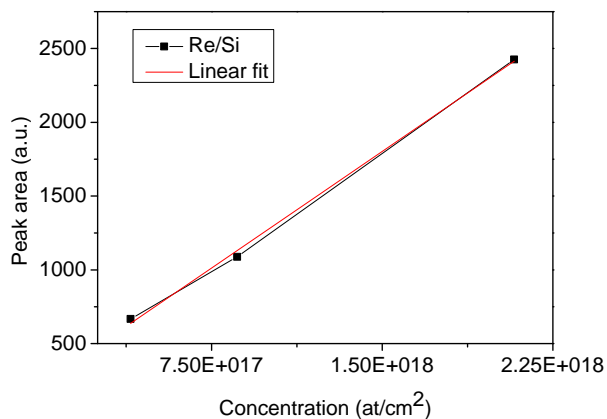*Fig. 5 Low energy micro-XRF Ni calibration curve using Ni deposited on different substrates*

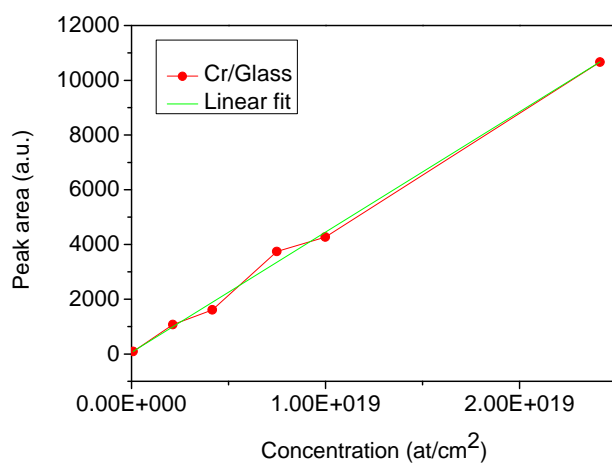*Fig. 6 Low energy micro-XRF Re calibration curve using Re deposited on Si substrates*

Fig. 7 Low energy micro-XRF Cr calibration curve using Cr deposited on Si and glass substrates

Figures 5-7 introduce the calibration curves for the Ni, Re and Cr atomic concentration correlated to Ni, Re, Cr micro-XRF Kα peak area.

Measuring the micro-XRF response in the 154 zones (1 cm analysis step), the 3D distribution graphs are presented in Figs. 8-10.
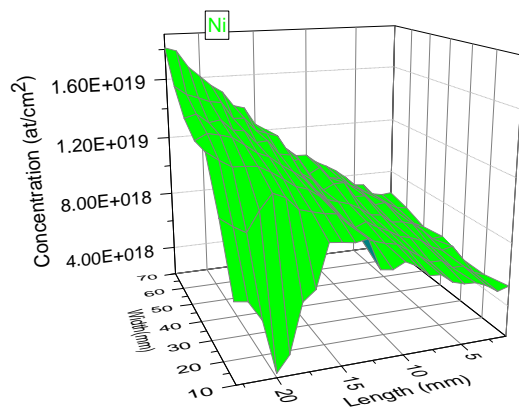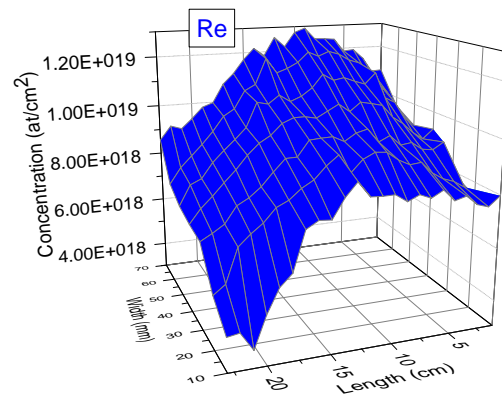

Fig. 8 3D mapping of Ni element

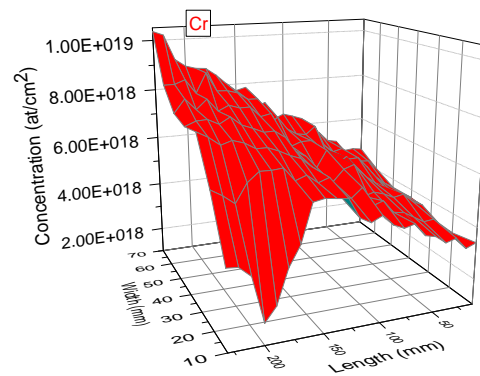*Fig. 9 3D mapping of Re element*

Fig. 10 3D mapping of Cr element

Using the data plotted in Fig.11 the appropriate zone where the relative concentration of the three elements was in the range of 25 – 50 at% was determined. The zone has a diameter of 5 +/- 1 cm.
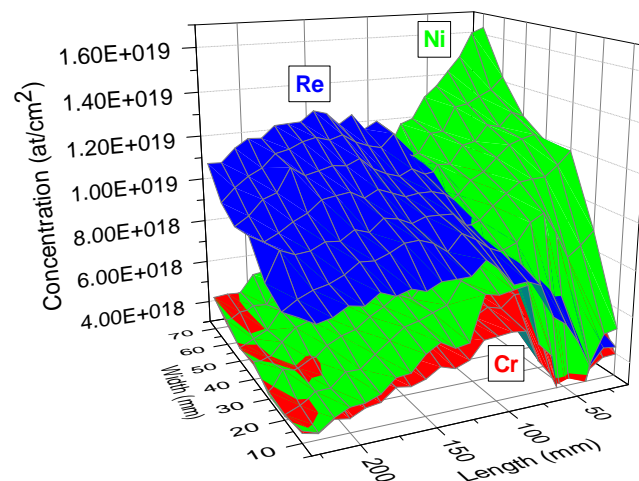

Fig. 11 Experimental distribution of the elements (Ni, Re, Cr) in at/cm 2 measured by micro-XRF calculated on an rectangular area of 240 mm x 90 mm

4. Conclusions

Using the thermionic vacuum arc method (TVA) Ni-Re-Cr mixed films were produced in order to obtain appropriate relative concentrations to be used as thermal barrier coatings. The prepared films were deposited on glass substrates of 240 mm X 90 mm.

The micro X-ray fluorescence (micro-XRF) method was used in surface mapping of the Ni-Re-Cr coated samples. Low energy micro X-ray fluorescence method was used to measure the atomic concentration (at/cm^2) for low thickness deposited layers (<5 μm).

Deposited layers with known thicknesses were prepared and used to perform precisely matching calibration curves for Ni, Re and Cr that describe the relationship between micro-XRF photon counts and the atomic concentration of the pure thin films.

The relative atomic concentrations of the Ni/Re/Cr alloys were found in the range of 25-50 at% in a central zone with a diameter of 5±1 cm. A 3D mapping of the relative concentration of the Ni-Re-Cr elements on the prepared sample was made.

Acknowledgements

References

[1] Y. Wang; S. Ohnuki, S. Hayashi, T. Yoshioka, M. Hara and T. Narita: Materials Transactions **48**, 127 (2007).
[2] K. Durst, M. Göken, Mat. Science and Engineering: A, **387–389**, 312 (2004).
[3] F. Lang and T. Narita, Intermetallics **15**, 599 (2007).
[4] C.T. Liu, X.F. Sun, H.R. Guan, Z.Q. Hu, Surf. Coat. Technol. **197**, 39 (2005).
[5] M. Fukumoto, Y. Matsumura, S. Hayashi , K. Sakamoto, R. Tanaka and T. Narita, Oxid. Met. **60**, 355 (2002) .
[6] A. Naor, N. Eliaz, E. Gileadi, Electrochimica Acta, **54**, 6028 (2009).
[7] C. T. Liu, X. F. Sun, H. R. Guan, Z. Q. Hu, Surf. Coat. Technol. **194**, 111 (2005).
[8] C. C. Surdu Bob, C. P. Lungu, I. Mustata and L. Frunza, J. Phys. D: Appl. Phys. **41**, 132001 (2008).
[9] C. P. Lungu, I. Mustata, V. Zaroschi, A. M. Lungu, A. Anghel, P. Chiru, M. Rubel, P. Coad G. F. Matthews, JET-EFDA contributors, Phys. Scr. **T128**, 157 (2007).
[10] C. P. Lungu, I. Mustata, G. Musa, V. Zaroschi, A. M. Lungu and K. Iwasaki, Vacuum, **76**, 127 (2004).
[11] R. Vladoiu, V. Ciupina, A. Mandes, M. Contulov, V. Dinca, P. Popov, C. P. Lungu, Romanian Reports on Physics **63**, 1053 (2011).
[12] I. Jepu, C. Porosnicu, I. Mustata, C. P.Lungu, V. Kuncser, M. Osiac, G. Iacobescu, V. Ionescu, T. Tudor, Romanian Reports in Physics **63**, 804 (2011).
[13] A. Marcu, C. M. Ticos, C. Grigoriu, I. Jepu, C. Porosnicu, A.M. Lungu, C.P. Lungu, Thin Solid Films, **519**, 4074 (2011).
[14] I. Tiseanu, T. Craciunescu, A. Möslang Fusion Engineering and Design, **84**(7–11), 1847 (2009).
[15] I. Tiseanu, T. Craciunescu, B. Pegourier, H. Maier, C. Ruset, M. Mayer, C. Dobrea, A. Sima, Phys. Scr. T **145**, 014073 (2011).
[16] I. Tiseanu, M. Mayer, T. Craciunescu, A. Hakola, S. Koivuranta, J. Likonen, C. Ruset, C. Dobrea, ASDEX Upgrade Team, Surface & Coatings Technology **205**, S192 (2011).
[17] I. Mustata, C. P. Lungu, C. C. Porosnicu, I. Jepu, V. Zaroschi; Descarcari electrice in gaze si vapori; Editura Universitara (2012).
[18] V. F. Kovalenko, Teplofiziceskie Protzessy i Elektrovakuumnye Pribory, Sovetskoe Radio, Moskva, 1975 (in Russian).
[19] A. Roth, Vacuum Technology, North-Holland, 1976.